Journal of Nuclear Materials 385 (2009) 456–460

Contents lists available at ScienceDirect

Journal of Nuclear Materials

journal homepage: www.elsevier.com/locate/jnucmat

High level nuclear waste glass corrosion in synthetic clay pore solution and retention of actinides in secondary phases

D. Bosbach *, B. Luckscheiter, B. Brendebach, M.A. Denecke, N. Finck

Institut für Nukleare Entsorgung (INE), Forschungszentrum Karlsruhe, P.O. Box 3640, 76021 Karlsruhe, Germany

ARTICLE INFO

PACS:
28.41kw
61.05.cj
91.67Pq

ABSTRACT

The corrosion of the simulated high level waste glass GP WAK1 in synthetic clay pore solution was studied in batch-type experiments at 323 and 363 K with special focus on the effect of high carbonate concentration in solution. The corrosion rate after 130 days was $<10^{-4}$ g m^{-2} d^{-1} – no significant effect of the carbonate was identified. During glass corrosion, crystalline secondary phases (powellite, barite, calcite, anhydrite and clay-like Mg(Ca,Fe)-silicates) were formed. To obtain a molecular level picture of radionuclide speciation within the alteration layer, spectroscopic methods have been applied including grazing incidence X-ray absorption spectroscopy (XAS) to study the structural changes in the coordination of uranyl upon alteration layer formation. The number of equatorial oxygen atoms increases from 4 in the bulk glass to 5 in the alteration layer. Furthermore, reduced coordination symmetry was found. Hectorite, a frequently observed secondary clay mineral within the glass alteration layer, was synthesized in the presence of trivalent f-elements (e.g. Eu) and structurally characterized using time-resolved laser fluorescence spectroscopy. Structural incorporation into the octahedral layer is indicated.

1. Introduction

The corrosion behaviour of high level nuclear waste (HLW) borosilicate glasses under repository relevant conditions has been studied for decades [1–3]. The potential release or retention of radionuclides including actinides and fission products has been demonstrated on the basis of long-term (up to 15 years) corrosion experiments. Nevertheless, the effect of carbonate in the ground water which may contact the waste matrix has not been the focus of glass corrosion studies. Furthermore, the molecular level binding mechanism of key-radionuclides to the corrosion products is still not well understood. Both aspects contribute uncertainties to predictions on HLW glass corrosion behaviour over geological time scales as required for the safety case of a nuclear waste repository system.

Here the focus has been on two aspects: (i) the corrosion behaviour of the German simulated HLW glass GP WAK1 (element release rates & formation of secondary phases) and (ii) speciation of U within the glass alteration layer and of Eu speciation associated with clay minerals coprecipitated under repository relevant conditions.

Batch type corrosion experiments were performed with the GP WAK1 glass. Element release and the formation of secondary alteration phases were quantified. X-ray absorption spectroscopy (XAS) was used as a non-destructive, element specific technique to characterize the electronic and geometric structure of U-bearing borosilicate glasses. Grazing incidence analysis provides structural information on the corrosion layer of the leached glass. This is compared to the bulk structure obtained from analysis of standard fluorescence mode spectra. Furthermore, the trioctahedral clay mineral hectorite, which has been frequently observed in HLW glass corrosion experiments, was synthesised in the presence of Eu(III) as a non-radioactive chemical analogue for the trivalent actinides. The hectorite associated Eu(III) was characterized with time resolved laser fluorescence spectroscopy (TRLFS) to identify the molecular level sorption mechanism.

2. Experimental

Batch type corrosion experiments were performed with the German simulated HLW glass GP WAK1 [4], which has a composition comparable to the COGEMA R7T7 glass, in the two synthetic clay solutions both with and without $NaHCO_3$ and calcite excess added to the solution to study the effect of carbonate on the release or retention of the various elements. Glass powder (grain size 71–100 μm, glass surface area to solution volume (S/V): 5000 m^{-1}) of the glass product GP WAK1 was reacted in tantalum lined autoclaves at 323 and 363 K for 14 up to 800 days under argon atmosphere. Aqueous solutions were prepared to mimic clay pore water as observed in the Opalinus clay [5] and the clay systems associated with the German Konrad site [6] (Table 1). The Konrad

* Corresponding author. Tel.: +49 7247 826048; fax: +49 7247 825983.
E-mail address: Dirk.Bosbach@ine.fzk.de (D. Bosbach).

0022-3115/$ - see front matter © 2008 Elsevier B.V. All rights reserved.
doi:10.1016/j.jnucmat.2008.12.044

Table 1
Chemical composition of the aqueous solutions used for glass corrosion experiments. The composition represents the composition of clay pore solution in the swiss Opalinus clay [5] and in the clays associated with the German Konrad site [6].

	Opalinus clay	Konrad site
pH	6.9	6.8
Na (mg L^{-1})	5750	59260
K (mg L^{-1})	223	242
Ca (mg L^{-1})	1240	11270
Mg (mg L^{-1})	559	2341
Si (mg L^{-1})	7.8	6.5
Cl^- (mg L^{-1})	11024	30.9
SO_4^{2-} (mg L^{-1})	2590	119620
F^- (mg L^{-1})	2.3	893
HCO_3^- (mg L^{-1})	98	73

water is salt-rich (high Na, Ca, and Mg concentration), whereas the Opalinus water is particularly rich in SO_4^{2-}. The synthetic clay solutions were prepared by dissolving a mixture of various Na-, K-, Mg-, and Ca-chlorides and of Mg- and Ca-sulfate (Opalinus clay water: $MgSO_4$: 2760, KCl: 423, Na_2SO_4: 576; NaCl: 14024; $CaCl_2$: 3430; NaF: 5.88; $NaHCO_3$: 134; Konrad water: $MgSO_4$: 1120; $MgCl_2$: 8286: KCl: 462; NaCl: 150540; $CaCl_2$: 31240; $AlCl_3$: 153; $NaHCO_3$: 134 [mg L^{-1}]). Furthermore, 4 g L^{-1} calcite was added in order to ensure saturation of the solution with $CaCO_3$ throughout the experiment. Each reaction vessel, except the vessels for the 14 and 60 days runtime, contained a GP WAK1 glass chip in order to study the formation of alteration products in detail. Further, an ironchip (Feinkorn-Baustahl 1.0566) was added in order to mimic the influence of the steel canister material on the glass corrosion, in particular with respect to the redox potential. Samples were taken after 14, 60, 130 days and after 1 and 2 years. For each runtime separate reaction vessels were used. Solution samples were filtered through a 0.45 μm filter, diluted with 0.1 M HNO_3 and analysed by ICP-MS and ICP-AES for B, Li, Cs and Si, Ca, Sr, Mo, Nd, Ce, U. Before sampling, the pH and *Eh* values of the solutions were determined by means of a pH electrode (Ross system) and a Pt electrode, respectively. The pH was measured with a pH electrode (Ross system) and the presented data (Fig. 1) are not corrected for liquid junction potential [7]. In case of Opalinus clay water the correction ΔpH is below 0.1 and in Konrad water at about 0.45. The alteration products on the added glass chips were analysed by SEM, EDX and XAFS.

Three glass chip samples were studied by X-ray absorption spectroscopy (XAS) as a non-destructive, element specific technique to characterize the electronic and geometric structure of U-bearing borosilicate glasses: a freshly prepared glass and two glasses after one year of leaching at 323 and 363 K in Opalinus clay water, respectively. Spectra were recorded at the INE-Beamline for Actinide Research [8] at the Ångstrømquelle Karlsruhe (ANKA), Forschungszentrum Karlsruhe (FZK), Germany. The U L_3-spectra of the leached samples were recorded in total external reflection geometry. Grazing incidence X-ray absorption fine structure (GI-XAFS) characterizes the surface layers, as the penetration depth of the X-ray photons is limited to a few nm [9]. GI-XAFS data were recorded with an incidence angle of approximately 0.1°. Seven spectra were averaged for each sample to improve the signal-to-noise ratio. A freshly prepared glass (bulk fresh) and the sample leached at 363 K (bulk leached) were also measured three times in standard fluorescence mode and averaged.

To be able to identify distinct uptake mechanisms associated with secondary clay minerals, hectorite was synthesized following a multi-step synthesis procedure [10] in the presence of Eu(III) (Mg:Eu ~ 9700:1) independently of the glass corrosion experiments. Also, a Eu(III)-containing precursor ($Mg(OH)_2$) was prepared for the same Mg:Eu ratio. Prior to TRLFS (time-resolved laser fluorescence spectroscopy) investigations, the Eu(III) doped hectorite was characterized by X-ray diffraction (XRD) and attenuated total reflectance – Fourier-transform infrared (ATR-FTIR) spectroscopy. No influence of Eu(III) coprecipitation on the clay mineral structure could be observed, as reported previously [11,12]. Low-temperature ($T < 20$ K) site-selective TRLFS was used to characterize different Eu(III) species formed during the coprecipitation with the magnesian smectite hectorite.

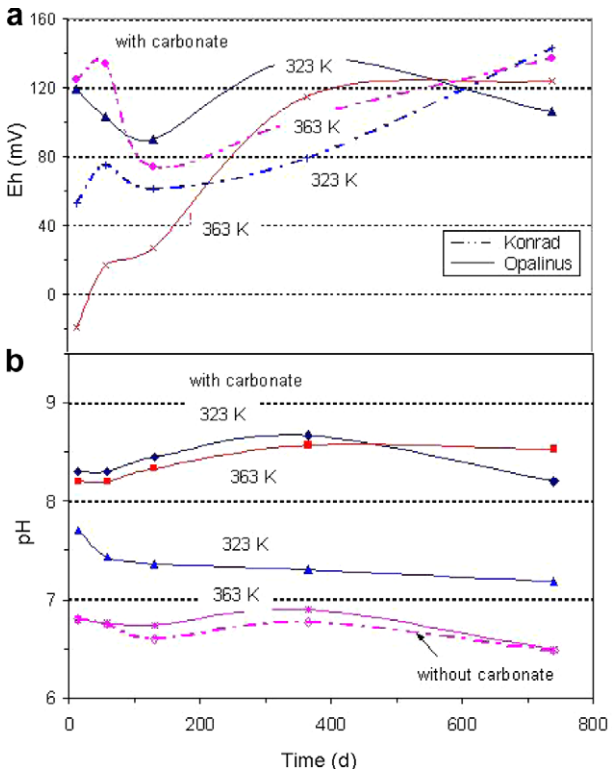

Fig. 1. (a) *Eh* evolution during the glass corrosion tests in Opalinus clay and Konrad water at 323 and 363 K in presence of carbonates. (b) pH evolution (not corrected) during the glass corrosion tests in Opalinus clay and Konrad water at 323 and 363 K in presence of carbonates.

3. Results and discussion

3.1. pH and Eh evolution during HLW glass corrosion

The evolution of pH in Opalinus clay and Konrad water during the corrosion tests at 323 and 363 K in solutions with added $NaHCO_3$ and calcite are shown in Fig. 1. In Opalinus water the pH increases slightly with time from 8.2 to about 8.5. In Konrad water the pH is significantly lower (even if correction ΔpH is regarded). At 363 K the pH decreases slowly with time from about 6.8–6.5 and at 323 K from 7.8 to 7.1 after 2 years. In solutions without calcite added, the evolution of pH is similar. Redox potential evolution is shown in Fig. 1. At the beginning of the corrosion the *Eh* values scatter between −20 and 140 mV. After 2 years corrosion time the *Eh* values in the various solutions are in the range between 95 and 140 mV. Even though the corrosion tests were performed under argon and in the presence of Fe-chips, the conditions are still slightly oxidising.

3.2. Corrosion behaviour in Opalinus clay water

The highest normalised mass loss is observed for Cs, B, Sr, and Mo (Fig. 2) as well as Li (not shown in Fig. 2). The release of these elements is similar and increases slowly with time. After 130 days,

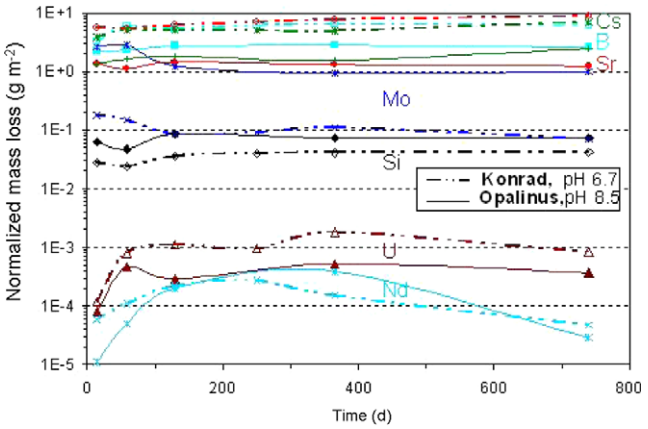

Fig. 2. Comparison of the release behaviour of various elements in Opalinus clay and Konrad water at 363 K in presence of carbonate.

their concentration remains almost constant and the glass corrosion rate approximates zero (rate detection limit $\leqslant 10^{-4}$ g m^{-2} d^{-1}). The mass loss of Si is significantly lower and saturation concentration at about 75 mg L^{-1} Si is reached after 14 days. Afterwards the Si concentration increases slowly to ~90 mg L^{-1}. Ca and Mg concentration in the solution decreased most likely as a consequence of sorption and/or precipitation of Mg- and Ca-silicates. The lowest mass loss is observed for U and Nd. An unexpectedly strong increase of Nd concentration after 1 year in the solution without added carbonates was observed, which we cannot explain at this stage. Besides Nd, there are only small differences in the release behaviour of the various elements in the solution with and without added $NaHCO_3$ and calcite. The release of Cs, Sr, Si, and Mo (and also of Li and B) is nearly identical in both solutions. In the presence of carbonates the release of Ce, Nd and U appears somewhat higher (factor 2) up to one year corrosion time. However, after 2 years the differences diminish. Apparently, carbonate ions in solution have only a minor effect on the release behaviour in Opalinus clay water within the time frame of our experiments. The release behaviour of the various elements and also the pH value at 323 and 363 K is similar (except for Si, Mo, and U), indicating a low effect of temperature on the glass dissolution under these conditions. At 323 K the Si concentration of 35–47 mg L^{-1} Si is clearly lower than at 363 K (75–90 mg L^{-1} Si), and also the U concentration is considerably lower at 323 K. Contrary to Si and U, the Mo release is even higher at 323 K by a factor of 3 after 130 days than at 363 K. As at both temperatures the pH in the solutions is nearly identical, no explanation can be given for the different Mo release at 323 and 363 K. Again, no remarkable effect of the added carbonate on the glass dissolution can be observed.

3.3. Corrosion behaviour in Konrad water

The pH in Konrad water is significantly lower than in Opalinus water – it decreases from 6.8 to 6.5 (Fig. 1). The lower pH in the $MgCl_2$-rich Konrad water can be explained by formation of OH-containing Mg-silicates (clay minerals) [13]. Again, the presence or absence of carbonates has nearly no effect on the glass corrosion behaviour. At 323 K, the saturation concentration of Si is clearly lower at about 16–21 mg L^{-1} Si compared to 30–50 mg L^{-1} Si at 363 K (Fig. 2). Contrary to Si, the release of Mo is much higher at 323 K. The higher release of Mo at 323 K is caused by the higher pH of 7.7 at the beginning of the corrosion test and the resultant higher solubility of molybdates (explained below). With increasing time the pH decreases to 7.1, and according to the decreasing solubility of molybdates, the Mo concentration decreases slightly with time. The amount of soluble elements released is by about a factor of two higher at 363 K after 2 years, whereas the release of Nd and U is similar at both temperatures.

Compared to Opalinus clay water, the Si saturation concentration and the Mo release is much lower in Konrad water. The lower Si concentration results from the high $MgCl_2$ concentration [14] and the lower release or concentration of Mo can be explained by the lower pH in Konrad water. The solubility of molybdates, e.g. powellite, is low between about pH 4 and 8. Above pH 8 the solubility of Mo increases strongly, which may explain the higher Mo concentration in Opalinus water at pH above 8. Due to the lower pH in Konrad water, the release of B, Cs, Sr, and also U is higher by about a factor of 2–3 compared to Opalinus clay water. However, the corrosion rates after 130 days are similar in both types of solutions. The normalised mass loss of Nd is also similar in both solutions. The concentrations of Nd and U are rather low between 1 and 3×10^{-7} mol L^{-1}.

3.4. Formation of crystalline secondary phases

In Opalinus clay water, all glass chips showed small tetragonal powellite ($CaMoO_4$) and barite ($BaSO_4$) crystals. In the powellite crystals rare earth elements could not be detected by EDS. On the glass chip corroded at 323 K newly formed rhombohedral calcite crystals were found in those solutions with added calcite. At 363 K aggregates of fine-grained, clay-like particles were detected consisting of Mg-silicates, each containing up to 5% Ca and 7% Fe. In a few cases, spherical crystals of Ca-phosphate and also bar-like anhydrite crystals were observed. After 1 year reaction time the amount of clay-like Mg(Ca,Fe)-silicates on the glass surfaces strongly increases in Opalinus clay water. In Konrad water, powellite crystals were found only at 363 K whereas barite in the form of small needle-like crystals was present on all glass chips investigated. Like in Opalinus clay water, clay-like Mg-silicates were found at 323 and 363 K, however their Ca content and above all the Fe content was much lower (below 2.5 and 1%, respectively) than in Opalinus water. Further, needle-shaped and small plates of anhydrite crystals were observed at 363 K but no calcite.

3.5. X-ray absorption spectroscopy (XAS) characterisation of U speciation within the glass alteration layer

The k^3-weighted extended X-ray absorption fine structure (EXAFS; $\chi(k)$) are presented in Fig. 3a and the corresponding Fourier transformed (FT) data is plotted in Fig. 3b. Spectra were analyzed using standard techniques described elsewhere [15]. Least-square fit results are summarized in Table 2 using a model of two O coordination shells. Results for the bulk samples are comparable to known uranyl containing compounds structures [16] with two short axial O distances (O1) and four further distant O atoms bound to U(VI) in the equatorial plane (O2). The U coordination structure in the glass bulk is not affected by leaching, as both bulk fresh and the bulk leached results are the same. Analysis of the GI-XAFS shows that U retains two shorter O1 distances within the corrosion layers. The number of O2 atoms increases from approximately four in the bulk to five in the corrosion layer. This finding is corroborated by the near edge (XANES) spectra (not shown). The most dominant feature, the so-called white line (WL), increases for samples GI 323 K and GI 363 K. This may indicate reduced U coordination symmetry in the corrosion layer. Similar trends have been reported for Hf(IV) sorbed onto mineral surfaces [9]. Both, the symmetry decrease and O2 number increase in the corrosion layer can be explained by additional coordinated water molecules within this layer. The FT spectra exhibit no contributions at R–Δ values beyond the U–O peak, indicating that neither U agglomerates are present in the bulk glass nor do secondary

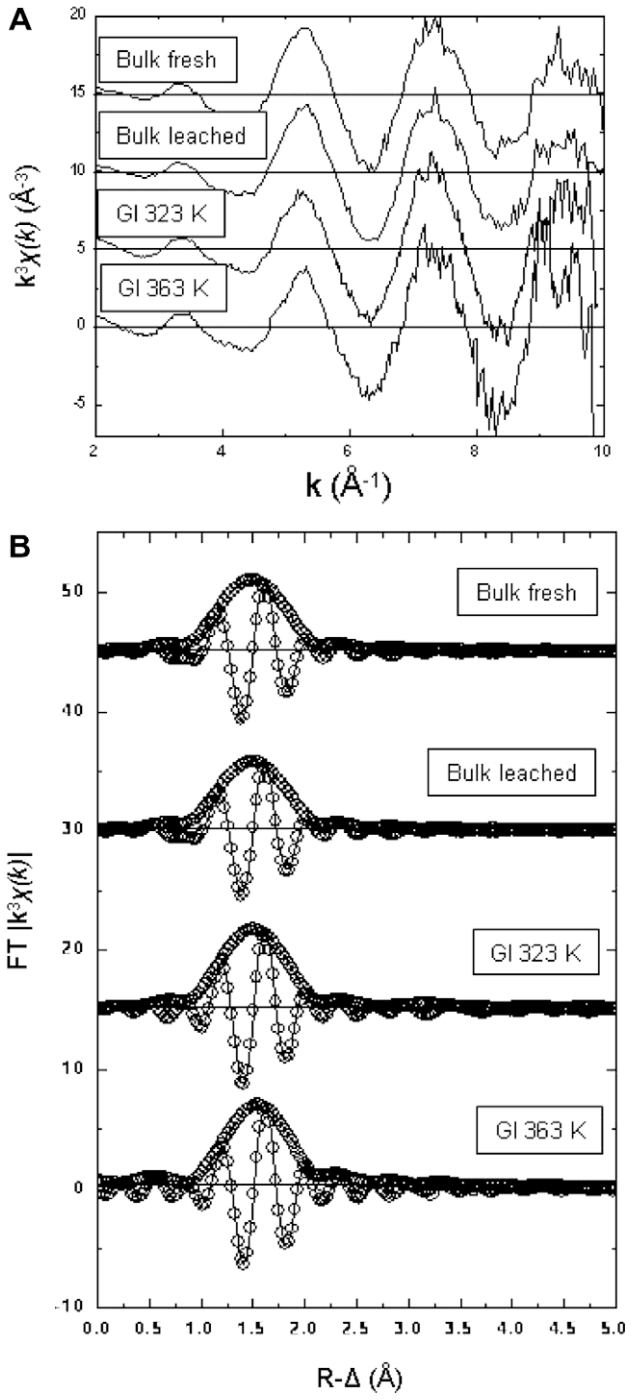

Fig. 3. (a) Measured uranyl L_3 k^3-weighted $\chi(k)$-functions. (b) Fourier transfroms of the data. Experimental functions are shown as lines and fit curved as symbols (see text for details).

U-phase form on the surface of the glass after leaching. This is in contrast to previous GI-XAFS investigations of the leaching behaviour of other borosilicate glasses [17], where the agglomeration of uranium oxides was reported.

3.6. Time-resolved laser fluorescence spectroscopy (TRLFS) investigation of europium(III) coprecipitated with the clay mineral hectorite

Eu(III) speciation during clay mineral formation was characterized by TRLFS measurements – independently of the glass corrosion experiments. TRLFS measurements were first carried out on the Eu(III)-containing $Mg(OH)_2$ (brucite) precipitate, which is the key precursor phase for the synthesis procedure used in this study. Excitation data suggested the presence of two species, suggested by a broad main peak and a second smaller one. Emission data (Table 3) confirmed the simultaneous presence of two species in the (Mg/Eu) hydroxide. One species has lost its first hydration sphere (minor component; lifetime 1700 ± 100 μs [18]). The second (major) species (lifetime 350 ± 30 μs) is bound to 2.5 ± 0.5 H_2O, corresponding alternatively to 5 ± 1 OH^- [19]. Ageing this precursor in the presence of silica completes the clay synthesis. The condensation of the silica tetrahedral sheet onto the precursor is the second key step in the coprecipitation with hectorite.

Excitation data of Eu doped hectorite (Fig. 4a suggest the presence of two Eu(III) species, indicated by a broad main peak. Emission data also suggest this result: two Eu(III) species are simultaneously detected (Fig. 3b, Table 3). One (minor) species is fully dehydrated (lifetime 1890 ± 100 μs), and the second (lifetime 580 ± 50 μs) is bound to 1.0 ± 0.5 H_2O [18], or alternatively to 2 ± 1 OH^- groups [19] in the first Eu(III) coordination shell. In brucite ($Mg(OH)_2$), the magnesium atom is in the centre of an octahedron of hydroxyls. Considering the hydration state of the main species detected in the Eu(III) doped brucite, we may hypothesize that Eu(III) ions are incorporated into the brucite lattice. The lanthanide ion surrounded by six hydroxyl groups may approximately replace Mg^{2+} in the octahedral sheet. The short-lived species (580 ± 50 μs) detected in the doped synthetic clay corresponds to Eu(III) bound to 1.0 ± 0.5 H_2O or 2 ± 1 OH^- groups in the first coordination shell. Obviously, water molecules were released from the forming hectorite as a consequence of the condensation of $[SiO_4]^-$ tetrahedra onto the pre-existing precursor. These 2 ± 1 OH^- quenchers present in the first Eu(III) coordination sphere are in accordance

Table 2
EXAFS structural parameters from first shell fits. R = interatomic distance; N = coordination number; σ^2 = Debye–Waller factor; ΔE_0 = relative shift in ionization energy, used as a global parameter for both O distances. The r-factor describes the overall goodness of fit, which is χ^2 divided by the degrees of freedom. A value equals 0.003 means that theory and data agree within 3%.

Parameter	Bulk fresh	Bulk leached	GI 363 K	GI 323 K
N O1	1.8(3)	1.8(3)	2.0(3)	2.1(2)
R O1 (Å)	1.77(2)	1.77(2)	1.79(1)	1.81(1)
σ^2 O1 (Å^2)	0.003(1)	0.003(1)	0.003(1)	0.003(1)
N O2	3.9(6)	3.6(6)	4.7(5)	5.2(3)
R O2 (Å)	2.21(3)	2.21(3)	2.18(2)	2.18(1)
σ^2 O2 (Å^2)	0.003(2)	0.003(2)	0.003(2)	0.003(2)
ΔE_0 (eV)	−4.4(6.4)	−3.1(7.1)	−8.7(5.4)	−8.5(3.1)
r-factor	0.0029	0.0030	0.0034	0.0016

Table 3
Fluorescence emission characteristics for several Eu(III) species/compounds. Uncertainties are ±0.5 H_2O/±1 OH^-. $^5D_0\rightarrow{}^7F_1/^5D_0\rightarrow{}^7F_2$ intensity ratios determined at excitation wavelength of ~580 nm.

Eu(III) species/compound	$^5D_0\rightarrow{}^7F_2$ /$^5D_0\rightarrow{}^7F_1$ intensity ratios	Lifetime (μs)	Proportion (%)	Comment
Eu^{3+}_{aquo}	1/8–1/4 (Plancque et al., 2002)	110 (±5)	100	9 H_2O
$(Mg,Eu)(OH)_n$	~2/1	350 (±30)	15	2.5 H_2O/5 OH^-[a]
		1700 (±100)	85	0 H_2O/OH^-[b]
Eu(III)-doped hectorite	~3/1	580 (±50)	55–65	1 H_2O/2OH^-[c]
		1890 (±100)	35–45	0 H_2O/OH^-[b]

[a] Eu(III) in a brucite octahedral environment.
[b] Dehydrated Eu(III) species.
[c] Eu(III) in a clay octahedral environment.

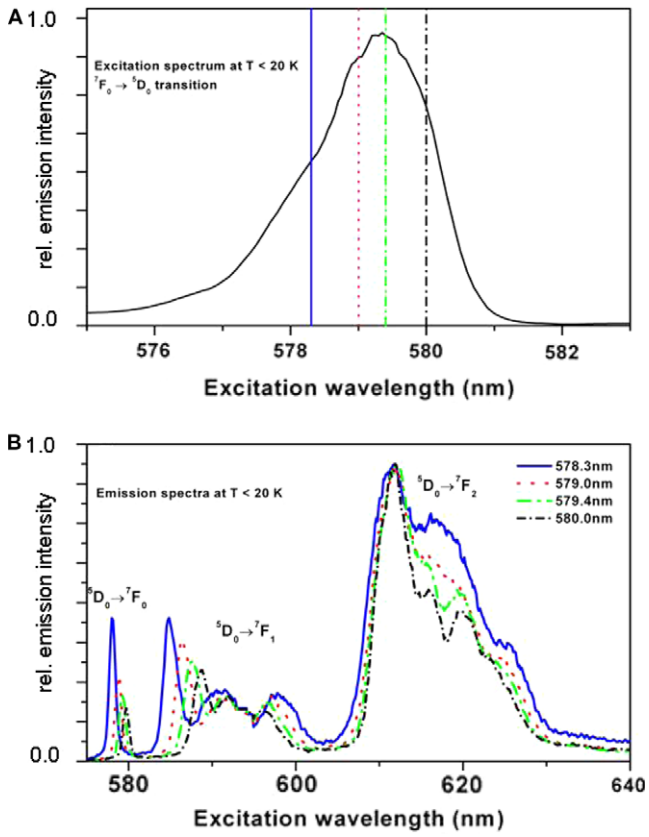

Fig. 4. Excitation (A) and emission (B) spectra for the Eu(III) doped hectorite. The emission spectrum shape is gradually modified with the excitation wavelength, indicating the presence of more than one Eu(III) species.

with the two OH groups at the unconnected corners of the $(Mg,Li,Eu)(O,OH)_6$-octahedra in the octahedral layer. Consequently, this indicates that the lanthanide substitutes for the cations present at the octahedral lattice site. Finally, for both samples, the formation of a Eu(III) surface complex can be excluded since a value of 4–5 water molecules in the first coordination sphere is usually found for lanthanide and actinide surface complexes [20].

Our results clearly show that macrosopic sorption processes with lanthanides and clay minerals involve in principle structural incorporation into the octahedral layer of clay minerals – in addition to adsorption and cation exchange reactions. Clearly, the neoformation of clay minerals opens the possibility to structurally incorporate trivalent f-elements (lanthanides and actinides) by coprecipitation. However, our results do not allow conclusions to be made about the thermodynamic stability of the f-element-doped clay mineral.

4. Summary and conclusions

Long-term corrosion tests with the simulated HLW glass GP WAK1 have been performed in two synthetic clay pore solutions based on the composition of the Opalinus clay water and Konrad water. The pH in Opalinus clay water ranged between 8.2 and 8.6 and in Konrad water between 6.8 and 6.5 over 2 years. The Si saturation concentration at 363 K amounts to about 90 mg L^{-1} in Opalinus water and about 50 mg L^{-1} in Konrad water. The lower saturation concentration of Si in Konrad water is related to the high $MgCl_2$ concentration. The release of the soluble elements Li, B, Cs, and Sr is rather similar both in Opalinus and Konrad water and remains nearly constant after 130 days (corrosion rates $\leqslant 10^{-4}$ g m^{-2} d^{-1}). The concentration of Mo depends strongly on the pH value in the solution. At the lower pH conditions in Konrad water, the Mo release is clearly lower than in Opalinus water. An effect of the added carbonates on the release of Ce, Nd, and U was not clearly visible. Also, the different temperatures of 323 and 363 K had only a small effect on the release of most of the elements investigated. The corrosion behaviour of the HLW glass in the clay pore solutions resembles the behaviour found in pure water and NaCl-rich solution at corresponding temperatures. In all these solutions the pH remains between about 7 and 9 and the pH value determines mainly, besides the temperature, the glass corrosion behaviour. The crystalline secondary phases found on the surface of the glass chips leached in Opalinus clay and Konrad water consist mainly of powellite, barite, calcite, anhydrite and above all of clay-like Mg(Ca,Fe)-silicates. EXAFS investigations indicate a reduced uranyl coordination symmetry in the corrosion layer. Both the symmetry decrease and increased number of equitorial O in the corrosion layer can be explained by additional coordinated water molecules within this layer. TRLFS measurements on Eu doped hectorite suggest the structural uptake of lanthanides (and trivalent actinides) into the octahedral layer of clay minerals.

Long-term batch-type glass corrosion experiments and state-of-the-art synthesis procedures for secondary alteration phases combined with modern spectroscopic techniques provide new insights into the HLW glass source term at molecular scales.

Acknowledgement

Eva Soballa is thanked for her help on the SEM. Finanical support of part of this study by the european integrated project NF-PRO and the european Network of Excellence ACTINET is gratefully acknowledged.

References

[1] P. van Iseghem, M. Aertsens, S. Gin, D. Deneele, B. Grambow, P. McGrail, D. Strachan, G. Wicks, A critical evaluation of the dissolution mechanism of high level watse glasses in conditions of relevance for geological disposal, in Contract FIKW-CT-2001-20140, European Commission, 2006.
[2] E. Vernaz, D. Gin, C. Jegou, I. Ribet, J. Nucl. Mater. 298 (2001) 27–36.
[3] W. Lutze, R.C. Ewing, Radioactive waste forms for the future, Amsterdam, North Holland, 1988.
[4] B. Luckscheiter, M. Nesovic, Waste Manage. 17 (1998) 429–436.
[5] M.H. Bradburry, B. Baeyens, Deviation of in-situ Opalinus clay porewater compositions from experimental and geochemical modelling studies, in NAGRA Technical Report, NAGRA, Switzerland, 1998.
[6] W. Brewitz, Eignungsprüfung der Schachtanlage Konrad für die Endlagerung radioaktiver Abfälle, Gesllschaft für Strahlen- und Umweltforschung: Neuherberg, Germany, 1982.
[7] B. Grambow, R. Müller, MRS Symposium Proc. (Pittsburg) 176 (1989) 229–240.
[8] M.A. Denecke, J. Rothe, K. Dardenne, H. Blank, J. Hormes, Phys. Scripta T115 (2005) 1001–1005.
[9] M.A. Denecke, J. Rothe, K. Dardenne, P. Lindquist-Reis, Phys. Chem. Chem. Phys 5 (2003) 939–944.
[10] K.A. Carrado, P. Thiyagarajan, K. Song, Clay Miner 32 (1997) 29–40.
[11] M. Spagnuolo, C.E. Martinez, A.R. Jacobson, P. Baveye, M.B. McBride, J. Newton Appl. Clay Sci. 27 (2004) 129–140.
[12] H. Pieper, D. Bosbach, P.J. Panak, T. Rabung, T. Fanghanel, Clay. Clay Miner. 54 (2006) 45–53.
[13] A. Abdelous, J.L. Crovosier, W. Lutze, B. Grambow, J.C. Dran, R. Müller, J. Nucl. Mater. 240 (1997) 100–111.
[14] B. Grambow, R. Müller, J. Nucl. Mater. 176 (1990) 229–235.
[15] B. Brendebach, R. Glaum, M. Funke, F. Reinauer, J. Hormes, H. Modrow, Zeitschr. Naturforsch. 60 (2005) 449.
[16] C. Den Auwer, E. Simoni, S. Conradson, C. Madic, Eur. J. Inorg. Chem. (2003) 3843–3851.
[17] G.N. Greaves, N.T. Barret, G.M. Antonini, F.R. Thomley, B.T.M. Willis, A. Steel, J. Am. Ceram. Soc. 111 (1989) 4313.
[18] W. Horrocks, D.R. Sudnick, J. Am. Chemi. Soc. 101 (1979) 334–340.
[19] R.M. Supkowski, W. Horrocks, Inorg. Chim. Acta 340 (2002) 44–48.
[20] T. Rabung, M.C. Pierret, A. Bauer, H. Geckeis, M.H. Bradburry, B. Baeyens, Geochimi. Cosmochimi. Acta 69 (2005) 5393–5402.